Layer-by-Layer Assembly of Polyelectrolytes in Nanopores

Halima Alem,[†] Françoise Blondeau,[†] Karine Glinel,[‡] Sophie Demoustier-Champagne,[†] and Alain M. Jonas*,[†]

Unité de physique et de chimie des hauts polymères, Université catholique de Louvain, Place Croix du Sud, 1, B-1348 Louvain-la-Neuve, Belgium, and UMR 6522, Polymères, Biopolymères, Membranes, CNRS-Université de Rouen, Bd Maurice de Broglie, F-76821 Mont-Saint-Aignan, France

Received February 6, 2007; Revised Manuscript Received March 5, 2007

ABSTRACT: We study the layer-by-layer (LbL) deposition of a pair of strong polyelectrolytes within the nanopores of track-etched membranes, for pore diameters ranging from ∼50 to 850 nm. The end-to-end distance of the polyelectrolyte chains in solution was varied from 10 to 50 nm by selecting polyelectrolytes of low and high molar mass and by playing with ionic strength. On flat model surfaces, a linear growth is obtained for all probed conditions and the growth increment is independent of molar mass and substrate nature. When LbL assembly is performed within nanopores, a very different picture of growth emerges, with increments of thickness per cycle of deposition being much larger than on flat surfaces (by factors as large as 100 in some cases), and no significant dependence on molar mass or ionic strength. These observations indicate that polyelectrolyte complexation occurs within a dense gel filling the whole nanopore, resulting from entanglement of the chains which are in a concentrated regime when passing in the confined space of the pore; upon drying, the gel collapses in a tube of wall thickness roughly proportional to its diameter. By using polyelectrolytes of lower molar mass, pore diameters as small as 50 nm could be filled, opening opportunities for the facile fabrication of LbL nanowires of very large aspect ratio.

Introduction

Among the different methods developed to build thin organic or hybrid films, the layer-by-layer (LbL) assembly of polyelectrolytes has emerged as a particularly versatile method to fabricate functional multilayered films.[1−8] LbL, which primarily exploits the electrostatic attraction between oppositely charged species alternately adsorbing on a surface from solution, has been used to prepare films on substrates of varying nature (metals, glass, silicon, polymers)[1] and of varying shape and size (flat macroscopic surfaces, micro-[9] or nanopatterned[10] surfaces, porous membranes,[11,12] colloids[13]), using a variety of compounds (synthetic polyelectrolytes and biological macromolecules,[1] dyes,[14] nanoparticles,[15] carbon nanotubes,[16] etc.). Other types of interaction than the electrostatic one, notably H-bonding[17] or specific complexation,[18] were subsequently demonstrated to be useful for LbL assembly, thereby widening further the applicability of the method.

Recently, Cohen et al.[19] reported on the fabrication of pH-responsive membranes by growing LbL multilayers of pH-sensitive polyelectrolytes inside the pores of membranes. Two research groups had previously shown the possibility to obtain nanotubes of polyelectrolyte multilayers by replicating the open porosity of membranes, a templating strategy initially proposed by Martin et al. in another context.[20] In a first example,[21] nanoporous polycarbonate track-etched membranes were immersed in the polyelectrolyte solutions, and the assembly occurred by the diffusion of the polyelectrolytes within the nanopores. In a second example,[22−25] alternated filtration of polyelectrolyte solutions through alumina track-etched membranes was used. In both cases, dissolving the template gave rise to well-defined nanotubes, and the successful incorporation of proteins in nanotubes was even demonstrated.[24]

Considering the wide range of functional polymers which can be used to grow LbL multilayers, from strong polyelectrolytes to weak responsive polyions, including DNA, proteins and nanoparticles, it becomes obvious that membrane-templated LbL assembly could open access to a wide variety of functional filamentary nanostructures, not mentioning obvious applications in responsive filtration. However, although LbL deposition was demonstrated to occur in nanopores, the details of the process itself are currently not understood. One may speculate that the confinement of chains in pores of small dimensions might affect considerably the growth mechanism of the multilayers, similarly to what was reported recently for multilayers adsorbing on nanopatches.[10] A support to this hypothesis is provided by experiments showing that the thickness of the walls of LbL-grown nanotubes differs significantly from the thickness of flat multilayers obtained under identical deposition conditions.[19,21,22] However, the reasons for this behavior are not known, as no systematic study of LbL assembly in nanopores was undertaken so far. Therefore, in the present work, we report on LbL assembly by alternate filtration of polyelectrolyte solutions through polycarbonate track-etched nanoporous membranes. The size of the chains in solution was systematically tuned by varying the ionic strength of the solutions and the molar mass of the polymers, and the resulting LbL thickness was investigated for a set of pore diameters ranging from 4 to 80 times the end-to-end distance of the polyelectrolyte chains in solution (corresponding to pores of 50−850 nm in diameter). We demonstrate that the growth process in nanopores indeed differs from the one on flat surfaces, even for pore diameters as large as 850 nm, and explain this behavior with a model based on polyelectrolyte complexation in confined spaces.

Experimental Section

Polyelectrolytes. The structures of the polycations and polyanions used in this study are presented in Figure 1. Two poly-

* Corresponding author. E-mail: alain.jonas@uclouvain.be.
[†] Unité de physique et de chimie des hauts polymères, Université catholique de Louvain.
[‡] UMR 6522, Polymères, Biopolymères, Membranes, CNRS-Université de Rouen.

10.1021/ma0703251 CCC: $37.00 © 2007 American Chemical Society
Published on Web 03/30/2007

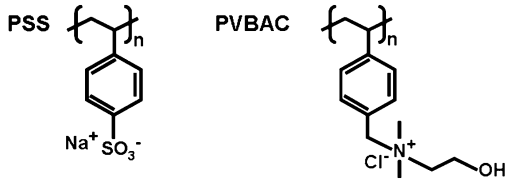

Figure 1. Chemical structures of the polyelectrolytes of this study.

(vinylbenzylammonium chloride) (polycationic PVBAC) samples of narrow polydispersity were synthesized from poly(vinylbenzyl chloride) (PVBC, Polymer Source, Canada) and purified as described elsewhere.[26] The low molar mass PVBAC sample, PVBAC−LM (M_w = 17 800 g/mol; polydispersity = 1.24), was obtained from a PVBC sample of M_w = 12 600 g/mol and 1.34 polydispersity index; the high molar mass sample, PVBAC−HM (M_w = 84 100 g/mol; polydispersity = 1.54), was synthesized from a PVBC sample of M_w = 60 000 g/mol and 1.54 polydispersity index. The degrees of quaternization were checked by elemental analysis and are 0.9 and 0.86 for PVBAC−LM and PVBAC−HM, respectively ($C_{13}NOClH_{19}$, $M_{monomer}$ = 240.7 g/mol. Anal. Calcd: C, 64.59; H, 8.34; N, 5.79; Cl, 14.66. Found for PVBAC−LM, partially hydrated: C, 56.90; H, 9.21; N, 4.51; Cl, 12.01. Found for PVBAC−HM, partially hydrated: C, 55.56; H, 8.92; N, 4.69; Cl, 7.86). A poly(styrene sodium sulfonate) (polyanionic PSS) sample of low molar mass, PSS-LM (M_w = 13 800 g/mol; polydispersity = 1.09), was obtained by the sulfonation of a polystyrene (PS) sample (Polymer Source, Canada; M_w = 8000 g/mol and 1.17 polydispersity index) with sulfur trioxide (SO_3) using Bock et al.'s protocol.[27] The rate of sulfonation was estimated by ^{1}H NMR to be 75% (400 MHz, in D_2O, δ in ppm. 1.5 (m, CH backbone); 6.7−6.9 (d, 2H, Ar−CH), 7.2−7.65 (d, 2H, Ar−CH), 4.9−5.3 (d, 0.25H, Ar−CH)). The high molar mass sample, PSS−HM (M_w = 75 300 g/mol; polydispersity = 1.01), was purchased from Polymer Source Inc. (Canada) and was used after dialysis with a membrane of 6000 cutoff.

The molar masses of PSS were measured in 0.1 M $LiNO_3$ with a size-exclusion chromatography system (two OHPAK SB 804 and 806 HQ columns in series with an OHPAK SB-G guard column, from Shodex Showa Denko K.K., Tokyo, Japan) coupled online to a multiangle light scattering detector (DAWN-EOS spectrophotometer from Wyatt Technology Inc., Santa Barbara, CA; laser wavelength : 632.8 nm) and a differential refractive index detector (ERC 7515A from Erma CR Inc., Tokyo, Japan). A similar system consisting of two Syncropak CatSEC 1000 and 100 columns (Synchrom, Inc. USA), a DAWN−F spectrophotometer (Wyatt Technology inc., Santa Barbara, CA) and a RID-6A refractive index detector (Shimadzu, Japan) was used for the characterization of PVBAC. The collected data were analyzed using the Astra 4.81.50 software package using 0.146 and 0.197 mL·g^{-1} as increments of index of refraction (dn/dC) for PVBAC and PSS, respectively.

Substrates Used for LbL Assembly. LbL assembly was performed on cleaned (100) silicon wafers (ACM, France), or on flat surfaces of poly(bisphenol A carbonate) (PC) for reference. The PC substrates were obtained by spin-coating a 10 g/L solution of PC (General Electrics Plastics, The Netherlands) in spectrometric grade CH_2Cl_2 (Acros) onto (100) silicon wafers previously cleaned in a piranha solution (H_2SO_4 (98%)/H_2O_2 (27%) 1/1 v/v. ***Caution!*** *piranha solutions react violently with organic materials and should not be stored in closed containers*). Before spin-coating PC, a layer of hexamethyldisilazane (HMDS, Aldrich) was spun-coated on the wafer, to provide a better adhesion of the PC film on the wafer. After spin-coating, the films were annealed at 190 °C for 4 h; they were then slightly hydrolyzed in 0.5 M aqueous NaOH (Acros) for 20 min, to mimic the hydrolysis step used to generate pores in PC track-etched membranes.[28] This step has the further advantage to introduce negative charges on the PC surface, due to the formation of phenolic end groups which are negatively charged at the pH used for LbL assembly (5.5).

For LbL assembly in nanopores, polycarbonate track-etched membranes of 21 μm thickness were used. These membranes were supplied by It4ip, Seneffe, Belgium (http://www.it4ip.be), and had different average pore diameters (57, 103, 128, 258, 482, 650, and 845 nm).

Layer-by-Layer Assembly. PSS and PVBAC aqueous solutions 10^{-2} M in repeat unit were used for LbL assembly. For some experiments, the ionic strength of the solutions was adjusted to 0.5 M NaCl (Acros). The water used in all experiments was purified by a Millipore system (Milli-Q water of 18.2 MΩ.cm resistivity). For flat surfaces, LbL assembly was performed by first immersing the substrates into the polycation solution for 10 min, followed by 15 immersion steps (of 1 sec. each) in a first bath of pure water, then by four immersions (5 s. each) and one immersion (15 s.) in two other baths of Milli-Q water. The substrates were dried in warm air after each adsorption/rinsing step. The adsorption/rinsing/drying step was repeated for the polyanion; then the whole process was cycled until the desired number of bilayers was obtained. A half-integer number of bilayers of polycation/polyanion indicates that the polycation is in the outermost layer. For LbL assembly in nanopores, the polycation solution was first filtered under a pressure of 4 bar through the membrane to form a first layer of the LbL wall in the pore. The top surface of the membrane was then washed with pure water to remove the cake of unfiltered material, and pure water was filtered three times through the membrane under a pressure of 4 bar, to rinse the inner walls of the pores. The polyanion solution was then filtered similarly, thereby building the second "layer". Cycling this procedure led to the formation of a polyelectrolyte complex on the inner walls of the pores. In the case of salt-added solutions, the same procedure was followed except that the solution used for rinsing the top surface of the membrane was also 0.5 M in NaCl. After LbL assembly, nanotubes were sometimes extracted for observation. In this case, the surface of the membrane was polished by powdered Al_2O_3 (mesh size, Aldrich) and rinsed in Milli-Q water. Dissolution in CH_2Cl_2 liberated the nanotubes, which were collected by filtration on poly(ethylene terephthalate) track-etch membranes, and rinsed five times with CH_2Cl_2 before observation.

Characterization Methods. *The thickness of flat films* was measured by ellipsometry with a Digisel rotating compensator ellipsometer from Jobin-Yvon/Sofie instruments (France), working at 632.8 nm. To compensate for systematic errors (imperfections and residual misalignment of optical components), measurements were carried out with the analyzer at +45° and −45° (with respect to the plane of incidence).[29] Because the index of refraction of native silicon oxide (1.46) is close to the one of (PVBAC/PSS) multilayers (1.53) at the wavelength of the measurements, the layer of native Si oxide cannot be distinguished from the organic multilayer film. Therefore, a model consisting of a single isotropic film on a flat substrate was used to fit the ellipsometric angles,[30] providing access to the total ellipsometric thickness from which the multilayer thickness was obtained by subtraction of the thickness of the native oxide (determined to be ∼1.5 nm from a series of measurements on bare Si wafers). The refractive index of silicon was taken to be $3.881 - j0.019$.[31] The effective refractive index of the total film was obtained from the ellipsometric measurements by fitting in the (ψ,Δ)-plane trajectories corresponding to samples of increasing thickness, neglecting film absorption which is small at the working wavelength of the ellipsometer. For LbL multilayers grown on PC films, again, the index of refraction of the PC film (1.58) is too close to the one of the PVBAC/PSS multilayers (1.53) to allow for a separation of the total thickness in its two components by single-wavelength ellipsometry. Therefore, the LbL thickness was obtained by subtracting the measured thickness of the bare PC film from the thickness measured for the total LbL/PC film, as described above.

The morphology of flat films was imaged by atomic force microscopy (AFM) in air with an Autoprobe CP from Thermiscopes. The images were recorded in intermittent-contact mode (IC-AFM) with Pointprobe Tapping-mode sensors (Nanosensors). A second-order flattening procedure (line by line) was performed on AFM images.

Table 1. Estimated Dimensions of the Polyelectrolyte Chains in the Solutions Used in the Present Study

			end−to−end rms distance, R_{EE}, nm	
sample	M_w	extended length, L, nm	salt−free	0.5 M NaCl
PSS−LM	13 800	19	16	10
PSS−HM	75 300	104	51	25
PVBAC−LM	17 800	19	16	10
PVBAC−HM	84 100	92	47	24

The morphology of LbL in nanopores was determined by transmission electron microscopy (TEM). For some samples, the PC membrane was dissolved in CH_2Cl_2; then the freed nanotubes were collected on carbon grids, rinsed, and imaged with a LEO 922 TEM operated at 200 kV. However, as perturbations of the morphology of the nanotubes due to the dissolution step were detected, transmission electron microscopy of the LbL multilayers within the pores was usually preferred. The membrane was first cryo-microtomed to obtain 100 nm thick slightly oblique sections of the membrane. Therefore, the membrane was fixed between two frozen drops of water and placed close to parallel to the cutting edge of a microtome diamond knife, which gave rise to thin sections almost parallel to the membrane. The microtomes were picked up on copper TEM grids and imaged with a LEO 922 TEM microscope operated at 200 kV. The pores appeared as ellipses in the microtomes, from which the smallest axis was taken as a measure of pore diameter. For each sample, about hundred different pores were measured and the average taken to obtain a statistically significant average pore diameter. By recording the average pore diameter of the membrane before ($\langle d_{PC} \rangle$) and after ($\langle d \rangle$) LbL deposition, the average thickness of the LbL assembly was obtained as $t_{LbL} = (\langle d_{PC} \rangle - \langle d \rangle)/2$.

Results and Discussion

Estimation of the Size of the Chains in Solution. The size of the polyelectrolyte chains in solution is an important parameter to estimate, since the degree of confinement may be evaluated from the ratio between the end-to-end distance of the chains and the diameter of the pores. For polyelectrolytes in salt-free solutions, the root-mean-square end-to-end distances (R_{EE}) were determined from the standard theory of polyelectrolyte solutions.[32,33] Due to counterion condensation,[34,35] the average distance between two ionized charges along the chain is the Bjerrum length ($l_B = \sim 0.73$ nm in water at room temperature), which allows us to neglect the exact degree of sulfonation or quaternization of the chains. At our pH of 5.5, the Debye screening length d_B, which is the average distance over which electrostatic interactions are exerted,[36] amounts to about 6.5 nm. Since this is much larger than the average distance between two ionized charges on the polymer backbones (less than 1 nm), the chains are in the persistent regime, where they are locally stiffened by electrostatic repulsion between charged monomers. In this regime, the persistence length, which is the distance over which orientational correlation between the units of the chains still exists, is the sum of a negligible chain-intrinsic contribution and of an electrostatic persistence length which arises from electrostatic repulsion.[32,33] In our conditions, the electrostatic persistence length was evaluated as $l_{p,e} = l_B d_B^2 \tau^2/4 = \sim 14.5$ nm, where τ is the linear charge density approximated to l_B^{-1}. The root-mean-square distances between chain ends were then computed from their known extended lengths L and from their persistence lengths l_p, using:[37]

$$R_{EE} = (2l_p(L - l_p[1 - \exp(-L/l_p)]))^{0.5} \quad (1)$$

The resulting values are reported in Table 1. These values should be taken as estimates only, since the electrostatic persistence length is a strongly dependent function of the Debye screening length, which is only known approximately.

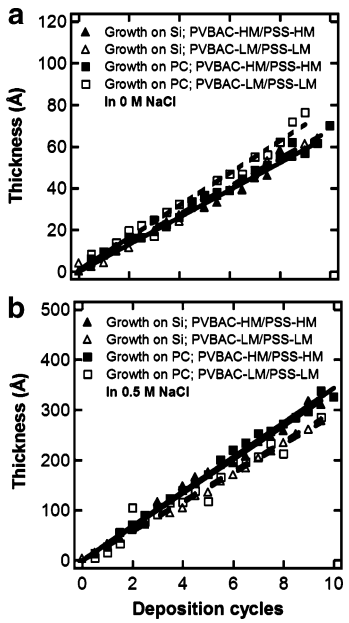

Figure 2. Thickness of LbL multilayers vs number of cycles of deposition, for PVBAC/PSS pairs of low (open symbols) and high (closed symbols) molar mass, deposited either on Si (triangles) or hydrolyzed PC (squares). Lines are drawn as a guide to the eye (continuous lines: high molar mass systems; dashed lines: low molar mass systems). Figures a and b refer to experiments performed in salt-free and 0.5 M NaCl solutions, respectively.

For polyelectrolytes in 0.5 M NaCl, the Debye screening length is only 0.4 nm, comparable to the lengths of the monomer units (0.25 nm). Therefore,[32,33] the chains are in the Gaussian regime, where they adopt random coil conformations with little electrostatic stiffening. Previous experimental work on PSS in salted solutions provided a value of 3.2 nm for the persistence length of PSS in 0.5 M NaCl,[38] which is indeed relatively close to the intrinsic persistence length of the PSS chain (0.9 nm).[39] This value of l_p was taken for both PSS and PVBAC, considering their close structural similarity, and was used to estimate R_{EE} in 0.5 M NaCl using eq 1 (Table 1).

The values reported in Table 1 show that the characteristic sizes of the chains range from ~10 to 50 nm, whereas membranes with pore diameters from 50 to 850 nm were used in this study, allowing to sample a large range of degrees of confinement. It should be stressed that, given the concentration of polyelectrolyte chains (0.01 M in repeat unit), all solutions are in the dilute regime where the chains do not overlap.

Growth of Multilayers on Flat Substrates. Flat LbL multilayers of different pairs of polyelectrolytes were first grown on Si wafers and hydrolyzed polycarbonate (PC), to obtain reference thicknesses. For all tested conditions, the growth of the multilayers was strictly linear over the probed range of deposition cycles (1−10) (Figure 2). The increments of thickness per cycle of deposition recorded for the different cases are reported in Table 2. In salt-free solutions, the increment ranges from 0.65 to 0.77 nm, which indicates that the chains adsorb in extremely thin layers. Because of electrostatic stiffening, strong polyelectrolytes at low ionic strength are known to adsorb flat on macroscopic surfaces, with only a limited number of short loops and tails dangling at the solid/liquid interface.[32] Therefore, it comes as no surprise that the increment of thickness is essentially independent of the nature of the substrate and of the molar mass.

Table 2. Average Increments of Thickness Per Cycle of Deposition for the Systems of This Study

pair of polyelectrolytes	NaCl concn (M)	increment on Si wafers (nm) [a]	increment on hydrolyzed PC films (nm) [a]
PVBAC−HM/PSS−HM	0	0.65 (0.02)	0.67 (0.02)
PVBAC−LM/PSS−LM	0	0.67 (0.02)	0.77 (0.03)
PVBAC−HM/PSS−HM	0.5	3.35 (0.07)	3.43 (0.06)
PVBAC−LM/PSS−LM	0.5	2.89 (0.04)	2.96 (0.15)

[a] The numbers in parentheses are the standard errors on the increment, as obtained from a linear fit.

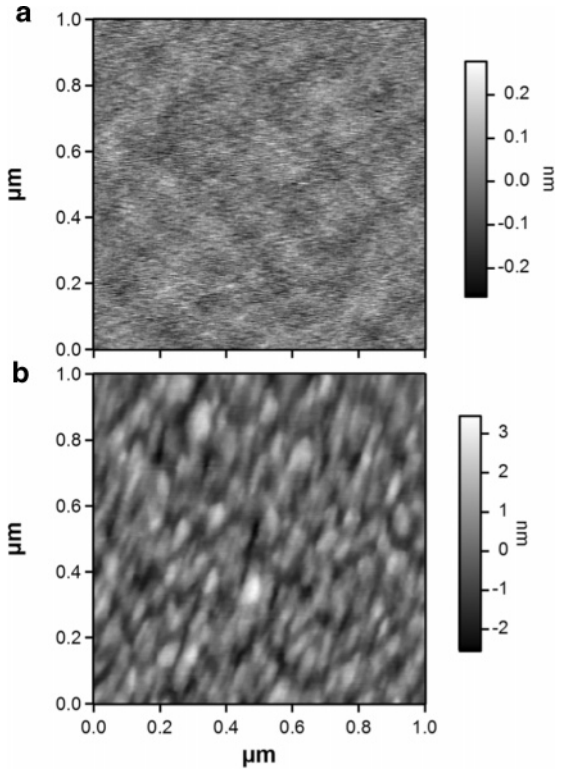

Figure 3. IC-AFM images of the surface of a PVBAC−LM/PSS−LM LbL multilayer (10 cycles) deposited on a Si wafer from (a) a salt-free solution or (b) a solution 0.5 M in NaCl.

The increments of thickness per cycle of deposition are also reported in Table 2 for salted PSS/PVBAC systems. A fivefold increase of thickness is observed upon addition of salt, due to the screening of the polyelectrolyte charges which results in a local crumpling of the chains and in the dominance of more coiled conformations. Consistent with the more coiled chain conformations, a slight dependence of thickness on molar mass can now be perceived: the increment of thickness increases by ∼15% for a ∼5-fold increase of molar mass. In contrast, no dependence on the nature of the substrate could be evidenced. The changes in chain conformation resulting from the addition of salt also translate into higher root-mean-square (rms) roughness, which increases upon salt addition from 0.1 nm (0 M in NaCl) to 0.8 nm (0.5 M in NaCl) (Figure 3).

Multilayers grown from salted solutions often exhibit nonlinear growth. There has been ample discussion in the literature regarding the origin of this behavior, which is usually ascribed to diffusion of polyelectrolytes down to a given depth into the growing film.[40−42] The perfectly linear growth of the PSS/PVBAC multilayers from salted solutions thus supports the notion that this specific pair of polyelectrolytes tends to form dense, impenetrable complexes even when grown from salted water. This makes them ideal candidates for our study of LbL growth in nanopores, since playing with the ionic strength of the solutions will only affect the conformations of the chains, not the mode of growth of the multilayers.

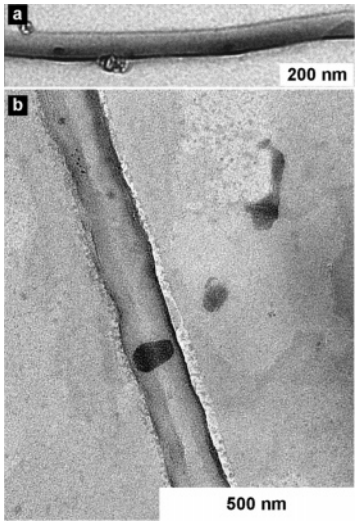

Figure 4. TEM images of (PVBAC−LM/PSS−LM)-based nanotubes grown in a membrane of 128 nm average pore diameter, from solutions devoid of salt. The tubes were grown to maximal filling of the pores.

Growth of Multilayers in Nanopores. Figure 4 presents TEM images of (PSS−LM/PVBAC−LM) nanotubes grown to the maximum filling (see below) in membranes of 128 nm average pore diameter. The tubes were found to be homogeneous in morphology over their whole length, demonstrating that the filling process is effective over the whole thickness of the membrane, even for such small pore diameters. Because of the distribution of pore sizes of the membranes, the tubes made in a given membrane differ slightly in diameter, being for instance 75 and 140 nm for the tubes shown in Figure 4a and b, respectively. In addition, in some instances, the tubes were seen to flatten when adsorbed on the TEM grids or to shrink after membrane removal. This generally prevented us to measure reliable dimensions from freed nanotubes. Therefore, LbL assembly in nanopores was studied by measuring on TEM microtomes the distribution of the diameters of the pores of the membranes before and after LbL filling. Typical distributions of pore sizes are shown in Figure 5 (all distributions are reported in the Supporting Information). From such distributions, the average thickness of the LbL assemblies could be easily derived.

The average thicknesses of the PSS−LM/PVBAC−LM and PSS−HM/PVBAC−HM pairs are shown in Figure 6, for one and two cycles of deposition from solutions 0 and 0.5 M in NaCl in pores of ∼250−850 nm average diameter (open and closed circles and squares). The average error bar on the multilayer thickness, derived from the statistics of the distributions, amounts to 6 nm. We also investigated LbL growth in pores of 57 and 103 nm diameter, concentrating on the low molar mass polyelectrolytes which have a typical end-to-end distance of 10−20 nm. For these cases, the deposition was cycled until the flow through the membrane dropped to zero. These points are collected as crosses in Figure 6a, and correspond to experiments performed in the presence and in the absence of salt, which provided essentially identical results.

Striking features emerge when considering Figure 6: first, the thickness of the multilayers after a single deposition cycle ranges from 50 to 120 nm, way above the 1−3 nm observed for flat multilayers, and considerably larger than even the

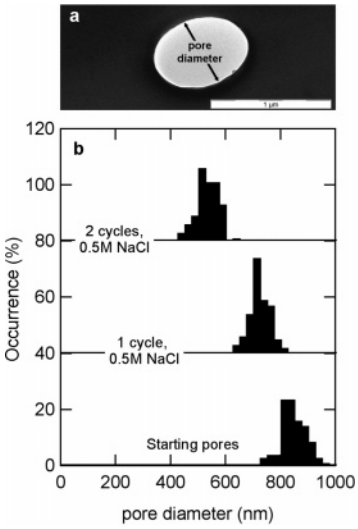

Figure 5. (a) TEM image of a cross section of a LbL-filled membrane (two cycles of PVBAC−LM/PSS−LM in 0.5 M NaCl; membrane of 845 nm average initial pore diameter). The small axis of the ellipse gives the diameter of the pore after filling. (b) Typical pore size distributions of a PC membrane before LbL assembly (bottom), and after 1 (middle) or 2 (top) cycles of deposition of PVBAC−LM/PSS−LM, from 0.5 M NaCl solutions. The top and middle curves are displaced vertically by 80 and 40%, respectively. These distributions were obtained from about hundred TEM cross sections such as shown in part a.

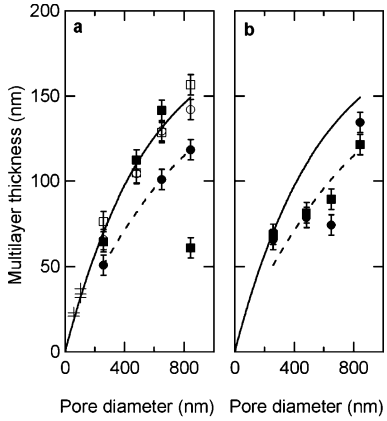

Figure 6. Thickness of LbL assemblies grown into nanopores of varying diameter. The multilayers were grown for one cycle (closed symbols) or two cycles (open symbols) from salt-free solutions (circles) or 0.5 M NaCl solutions (squares). The crosses refer to samples grown until the flow through the membrane dropped to zero. The left and right panels show results for low and high molar mass polyelectrolytes, respectively (PVBAC−LM/PSS−LM and PVBAC−HM/PSS−HM pairs, respectively). The continuous line in the left panel is the curve of maximal thickness attainable for the low molar mass system (see text); the dashed line is the thickness of the low molar mass system after one cycle of deposition in the absence of salt. To ease comparison, these curves are also drawn in the right panel.

extended lengths of the chains for some systems. Second, the thickness depends strongly on pore diameter, but little on molar mass (compare Figure 6a and Figure 6b) or ionic strength (compare squares and circles in Figure 6), indicating that the size of the polyelectrolyte chains in the starting solutions is of little importance. Third, the thickness of the multilayers after two cycles of deposition is usually only slightly larger than, and in some cases even identical to, the one obtained after one cycle of deposition only (compare closed and open symbols in Figure 6a). In addition, the curve of thickness vs pore diameter recorded for two cycles of deposition in pores of diameter larger than 250 nm nicely merges with the curve of thickness recorded when cycling was performed in the smaller pores until the flow through the membrane dropped to zero (crosses in Figure 6a). This shows that the pores are already completely filled by the multilayer after two cycles of deposition only, and that in most cases one cycle is almost sufficient to fill the pores.

At this stage, one should be aware that polyelectrolyte multilayers swell significantly when immersed in water. The degree of swelling, here defined as the ratio between the swollen and dry thickness, depends strongly on the nature of the polyelectrolytes and on the presence of salt, and ranges between 1.2 and 4 for most synthetic polyelectrolytes.[43,44] Therefore, when a swollen multilayer completely fills a pore, its thickness after drying will nevertheless be lower than the pore radius.

From the data points shown in Figure 6a, it is possible to define a curve of maximal filling in the swollen state. This curve, shown as a continuous line in Figure 6a, passes through the data points for which one and two cycles of deposition result in an identical multilayer thickness, and through the data points for which the flow through the membrane dropped to zero. The maximal filling depends linearly on pore diameter below 250 nm, then progressively saturates. The linear dependence may be easily understood since the mass conservation for a pore-filling LbL assembly before and after drying-induced collapse requires that :

$$\pi d^2/(4\alpha) = \pi d^2/4 - \pi(d - 2t_{\mathrm{LbL}})^2/4 \qquad (2)$$

where d is the pore diameter, t_{LbL} the thickness of the mutilayer after drying-induced collapse, and α the degree of swelling of the polyelectrolyte complex in the pore. Hence, the thickness of the dry multilayer after collapse is :

$$t_{\mathrm{LbL}} = d/2(1 - (1 - 1/\alpha)^{1/2}) \qquad (3)$$

which corresponds to a linear variation of multilayer thickness with pore diameter, provided the degree of swelling is constant. For pore diameters below 250 nm, the experimental slope is 0.26 (Figure 6a), corresponding to a degree of swelling $\alpha = 1.3$, which is in the range of published values for the degree of swelling of multilayers.[43,44] For larger pores, the experimental relationship deviates from linearity, indicating that the less confined systems swell more, with a degree of swelling of 1.7 computed for the multilayers completely filling the pores of ~850 nm diameter.

The rapid filling of the pores, which corresponds to unexpectedly large increments of multilayer thickness per cycle of deposition, and the insensitivity of the thickness to molar mass and ionic strength of the solutions, indicate that the mode of growth of the multilayers in the nanopores is fully different from what occurs on flat surfaces and that the sizes of chains in the starting dilute solutions is not a relevant parameter in the final structure. This points to a model into which chains entangle during their passing through the pores, due to a locally increased concentration, and make a dense gel filling almost completely the cavity. In the pores, the chains are thus no more in a dilute regime, but in a more concentrated regime where the end-to-end distance is not the proper characteristic size of the system, and where they pile up into the nanopores. Obviously, the pressure which is applied in order to force the chains to enter in the nanopores may be a factor favoring chain piling in the nanopores. The role of this parameter was not investigated here; however, as stated in the Introduction, larger than expected wall thicknesses were also reported by others, who did not apply pressure during LbL assembly in nanopores.[21] This suggests

that the observations reported here may be quite general for LbL assembly in nanoporous media.

With this model in mind, it becomes possible to discuss some minor features of the results displayed in Figure 6. However, when so doing, one should keep in mind that the dry thickness values reported in Figure 6 should be more appropriately be seen as masses of polyelectrolyte adsorbed in the pores, since the polyelectrolyte complexes may swell to various degrees in the pores. For instance, multilayers based on low molar mass polyelectrolytes (PVBAC−LM/PSS−LM) display a dry thickness slightly lower than the maximum filling when grown for one cycle in the absence of salt (dashed line in Figure 6a). This may thus correspond to pores filled with a gel of slightly larger degree of swelling, which would be made denser in the next cycle of deposition; or to truly incompletely filled pores in the swollen state, which would be filled in the next step of the process. It is also interesting to note that for high-molar mass systems, the thickness of the multilayer is identical after one cycle of deposition whether salt is added or not to the solutions (Figure 6b, closed circles and squares), while this is not the case for the low molar mass system (Figure 6a, same symbols). This may be due to a slightly lower maximal filling attainable for the high molar mass system, due to the overall larger size of the chains. Finally, one sample lies significantly below the curve of maximal filling, namely the low molar mass-based system grown for one cycle in the larger pores (850 nm) from a solution 0.5 M in NaCl. This corresponds to the larger ratio of pore diameter to chain end-to-end distance that was used in our experiments (about 85). Apparently, for this condition, the chains would not completely fill the pores, although the multilayer thickness is still way larger than for a flat multilayer. This sample thus testifies for the layer-by-layer nature of the film assembly in larger pores, which can be pursued upon cycling the process. One would expect that for even larger pores, a progressive return to the situation of flat multilayers would be attained.

Conclusions

We have studied the layer-by-layer deposition of strong polyelectrolytes (PVBAC/PSS) within the nanopores of track-etched membranes. Pore diameters were ranging from ∼50 to 850 nm, and the dimensions of the polyelectrolyte chains in solution were varied from 10 to 50 nm (rms end-to-end distance) by selecting polyelectrolytes of low and high molar mass, and by playing with ionic strength. Preliminary experiments on model flat surfaces indicated that a linear growth was obtained for all probed conditions, and that the growth increment of this specific system was independent of molar mass and substrate nature. This shows that the PVBAC/PSS system is a rather robust system for LbL assembly, devoid of the intricacies often reported for multilayers made from weak polyelectrolytes or biopolyelectrolytes.

When LbL assembly was performed within the nanopores, a very different picture of growth emerged, with increments of thickness per cycle of deposition being much larger than on flat surfaces (by factors as large as 100 for some cases). No significant dependence of this increment was found on the molar mass of the polyelectrolytes and on the ionic strength of the solutions, indicating that the size of the chains in the starting solutions is of little importance for this process. In contrast, the thickness of the LbL assemblies depends strongly on the pore diameter, being proportional to pore diameter at low diameter, then progressively deviating from this relationship for diameters above 250 nm. In addition, maximum filling of the pores (in solution) was almost reached after one cycle of deposition, except for the larger pores and the smaller chains. These observations strongly suggest that polyelectrolyte complexation occurs within a dense gel filling the whole nanopore, resulting from the entanglement of chains in the confined space of the pore; upon drying, the gel collapses in a tube of wall thickness directly proportional to its diameter. Deviations from linearity results from slightly different degrees of swelling of the multilayers.

The mode of growth of LbL assemblies within nanopores is thus fully different from the one of regular, flat LbL multilayers. As a result, one may expect significant differences of structure and properties between nanoconfined and flat LbL multilayers, although this is a domain which still remains to be explored in detail. Nevertheless, these systems offer exciting opportunities for the synthesis of nanowires down to very small dimensions, as was demonstrated here by the possibility to fill membranes of pore diameter as small as 50 nm.

Acknowledgment. The authors wish to thank Pascale Lipnik for help with cryomicrotomy. Financial support by the Belgian Federal Public Planning Service Science Policy (Inter-University Attraction Poles SC^2 and FS^2) and by the Belgian National Fund for Scientific Research (FNRS) is gratefully acknowledged. S.D.-C. is a Research Associate of the FNRS.

Supporting Information Available: Figures of pore size distribution before and after LbL filling. This material is available free of charge via the Internet at http://pubs.acs.org.

References and Notes

(1) Lvov, Y. M.; Decher, G. *Crystallogr. Rep.* **1994**, *39*, 628.
(2) Decher, G. *Science* **1997**, *277*, 1232.
(3) Bertrand, P.; Jonas, A.; Laschewsky, A.; Legras, R. *Macromol. Rapid Commun.* **2000**, *21*, 319.
(4) Hammond, P. T. *Curr. Opin. Colloid Interface Sci.* **2000**, *4*, 430.
(5) Decher, G.; Schlenoff, J. editors. *Multilayer Thin Films*; Wiley: Weinheim, Germany, 2003.
(6) Schönhoff, M. *J. Phys. Cond. Matter* **2003**, *15*, R1781.
(7) Arys, X.; Jonas, A. M.; Laschewsky, A.; Legras, R. In *Supramolecular Polymers*, 2nd ed.; Ciferri, A., Ed.; Marcel Dekker: New York, 2005; p 651.
(8) Klitzing, R. v. *Phys. Chem. Chem. Phys.* **2006**, *8*, 5012.
(9) Hammond, P. T.; Whitesides, G. M. *Macromolecules* **1995**, *28*, 7569.
(10) Pallandre, A.; Moussa, A.; Nysten, B.; Jonas, A. M. *Adv. Mater.* **2006**, *18*, 481.
(11) van Ackern, F.; Krasemann, L.; Tieke, B. *Thin Solid Films* **1998**, *327/329*, 762.
(12) Harris, J. J.; Stair, J. L.; Bruening, M. L. *Chem. Mater.* **2000**, *12*, 1941.
(13) Caruso, F.; Caruso, R. A.; Möhwald, H. *Science* **1998**, *282*, 1111.
(14) Cooper, T. M.; Campbell, A. L.; Crane, R. L. *Langmuir* **1995**, *11*, 2713.
(15) Fendler, J. H. *Chem. Mater.* **1996**, *8*, 1616.
(16) Mamedov, A. A.; Kotov, N. A.; Prato, M.; Guldi, D. M.; Wicksted, J. P; Hirsch, A. *Nat. Mater.* **2002**, *1*, 190.
(17) Sukhishvili, S. A. *Curr. Opin. Colloid Interface Sci.* **2005**, *10*, 37.
(18) Serizawa, T.; Hamada, K.; Kitayama, T.; Fujimoto, N.; Hatada, K.; Akashi, M. *J. Am. Chem. Soc.* **2000**, *122*, 1891.
(19) Lee, D.; Nolte, A. J.; Kunz, A. L.; Rubner, M. F.; Cohen, R. E. *J. Am. Chem. Soc.* **2006**, *128*, 8521.
(20) Hulten, J. C.; Martin, C. R. In *Nanoparticles and Nanostructured Films*; Fendler, J. H., Ed.; Wiley-VCH: Weinheim, Germany, 1998; Chapter 10.
(21) Liang, Z.; Susha, A. S.; Yu, A.; Caruso, F. *Adv. Mater.* **2003**, *15*, 1849.
(22) Ai, S.; Lu, G.; He, Q.; Li, J. *J. Am. Chem. Soc.* **2003**, *125*, 11140.
(23) Lu, G.; Ai, S.; Li, J. *Langmuir* **2005**, *21*, 1679.
(24) Tian, Y.; He, Q.; Cui, Y.; Li, J. *Biomacromolecules* **2006**, *7*, 2539.
(25) Li, J.; Cui, Y. *J. Nanosci. Nanotechnol.* **2006**, *6*, 1552.
(26) Nicol, E.; Habib-Jiwan, J.-L.; Jonas, A. M. *Langmuir* **2003**, *19*, 6178.
(27) Valint, P. L. Jr.; Bock, J. *Macromolecules* **1988**, *21*, 175.
(28) Ferain, E.; Legras, R. *Radiat. Meas.* **2001**, *34*, 585.

(29) Kleim, R.; Kuntzler, L.; El Ghemmaz, A. J. *J. Opt. Soc. Am. A* **1994**, *11*, 2550.
(30) Azzam, R. M. A.; Bashara, N. M. *Ellipsometry and Polarized Light*, North-Holland: Amsterdam, 1977.
(31) Apnes, D. E.; Studna, A. A. *Phys. Rev. B* **1983**, *27*, 985.
(32) Netz, R. R.; Andelman, D. *Phys. Rep.* **2003**, *380*, 1.
(33) Mandel, M. In *Encyclopedia of Polymer Science and Engineering*, 2nd ed.; Mark, H. F., Bikales, N. M., Overberger, C. G., Menges, G., Ed.; John Wiley & Sons: New York, 1988; Vol. 11, p 739.
(34) Manning, G. S. *J. Chem. Phys.* **1969**, *51*, 924.
(35) Manning, G. S.; Ray, J. *J. Biomol. Struct. Dyn.* **1998**, *16*, 461.
(36) Butt, H.-J.; Graf, K.; Kappl, M. *Physics and Chemistry of Interfaces*; Wiley-VCH: Weinheim, Germany, 2003.
(37) Grosberg, A. Y.; Khokhlov, A. R. *Statistical Physics of Macromolecules*; American Institute of Physics: New York, 1994.
(38) Spiteri, M. N.; Boué, F.; Lapp, A.; Cotton, J. P. *Phys. Rev. Lett.* **1996**, *77*, 5218.
(39) Borisov, O. V. *J. Phys. II* **1996**, *6*, 1.
(40) Picart, C.; Mutterer, J.; Richert, L.; Luo, Y.; Prestwich, G. D.; Schaaf, P.; Voegel, J.-C.; Lavalle, P. *Proc. Natl. Acad. Sci. U.S.A.* **2002**, *99*, 12531.
(41) Porcel, C.; Lavalle, P.; Ball, V.; Decher, G.; Senger, B.; Voegel, J.-C.; Schaaf, P. *Langmuir* **2006**, *22*, 4376.
(42) Salomaeki, M.; Vinokurov, I. A.; Kankare, J. *Langmuir* **2005**, *21*, 11232.
(43) Dubas, S. T.; Schlenoff, J. B. *Langmuir* **2001**, *17*, 7725.
(44) Miller, M. D.; Bruening, M. L. *Chem. Mater.* **2005**, *17*, 5375.

MA0703251